Chemical Engineering Journal 149 (2009) 110–117

Contents lists available at ScienceDirect

Chemical Engineering Journal

journal homepage: www.elsevier.com/locate/cej

Nonequilibrium dynamic modeling of carbon dioxide absorption by partially carbonated ammonia solutions

Ahad Ghaemi[a], Shahrokh Shahhosseini[a,*], Mohammad Ghanadi Maragheh[b]

[a] *Process Simulation and Control Research Laboratory, Department of Chemical Engineering, Iran University of Science and Technology, P.O. Box 16765-163, Narmak, Tehran, Iran*
[b] *Nuclear Science Research School, Nuclear Science and Technology Research Institute, P.O. Box 14155-1339, Amirabad, Tehran, Iran*

ARTICLE INFO

Article history:
Received 20 May 2008
Received in revised form 1 October 2008
Accepted 3 October 2008

Keywords:
Nonequilibrium stage modeling
Reactive absorption
Dynamic simulation
Carbon dioxide

ABSTRACT

In this research, a nonequilibrium dynamic stage model has been developed for reactive absorption of carbon dioxide by carbonated ammonia solutions. The model considers mass transfer between gas and liquid phases in both directions employing dynamic film model theory. Experimental data of carbon dioxide reactive absorption by partially carbonated ammonia solution has been used to validate the model. The data were obtained from a pilot plant absorption column. The model equations were discretized in column height direction. Simulations were performed, while either a film model or an enhancement factor was incorporated into the process model. The model predictions for both cases were compared with the experimental data. The comparison showed that simulation results were more accurate when film model has been used.

1. Introduction

Elimination of impurities from flue gases of many industries such as steel production, chemical and petrochemical manufacturing, and cement production is an important operation. Since CO_2 is regarded as a major greenhouse gas, its removal is well justified. Several technologies such as absorption by chemical solvents, membrane separation, and CO_2 fixation by microbes have developed for CO_2 removal [1–7]. CO_2 absorption by chemical solvents appears to be effective and practical. CO_2 absorption by amines is an important process since they react rapidly with CO_2. The reaction between amines and CO_2 brings some advantages such as increasing absorption rate of CO_2, absorption in low pressure. Absorption and reactions of CO_2 with amines have been extensively studied both theoretically and experimentally during last decades [8–19].

Packed columns are mostly used in gas absorption processes due to their high efficiency compared to other alternatives [1,15]. Several mathematical models with different complexity and accuracy have been proposed for reactive absorption in the literature [20–30]. In these models the column is divided into some theoretical stages. Each stage includes both gas and liquid phases. Two kinds of models have been reported; equilibrium and nonequilibrium stage models [21,22,31,32]. Due to some unrealistic assumptions in equilibrium stage models, they have been proved to be mostly inadequate to describe reactive separation processes [22].

Mass and heat transfer are actually rate phenomena driven by chemical potential and temperature gradients, respectively. Moreover, one of the important characteristics of reactive separation processes is that the reaction range widely changes from instantaneous to very slowly. Therefore a number of nonequilibrium models have been developed [33–38,20,23–29].

Nonequilibrium models are more rigorous and complex than equilibrium models, especially rate-based models, in which actual rates of multicomponent mass and heat transfer and chemical reactions are directly taken into the account. Rate-based models have been developed applying film modeling approach for which there are lots of experimental correlations in the literature [22,27,29].

Film model theory has been used in the majority of reported models. These models assume mass transfers only from gas phase to liquid phase, whereas in the real processes it happens in both directions.

Dynamic nonequilibrium models of reactive separation problems have reportedly been solved assuming steady-state descriptions of the interfacial and film phenomena [38,39,30,31]. Therefore in this work the process of reactive CO_2 absorption by partially carbonated ammonia solution in a packed column was modeled using unsteady-state film model and assuming mass flows in both directions (liquid and gas).

2. Modeling

Mathematical models of reactive separation processes usually include a few equations to compute heat and mass transfer rates between bulks and films of both phases. In these models

---

* Corresponding author. Tel.: +98 21 73912701.
E-mail address: shahrokh@iust.ac.ir (S. Shahhosseini).

1385-8947/$ – see front matter © 2008 Elsevier B.V. All rights reserved.
doi:10.1016/j.cej.2008.10.020

Nomenclature

a	specific packing surface (m^2/m^3)
A	cross-sectional area (m^2)
C	molar concentration (mol/m^3)
E	specific energy holdup (J/m)
G	gas phase molar flow rate (mol/s)
h	molar enthalpy (J/mol)
H	specific enthalpy (J/mol)
K	vapor–liquid equilibrium constant
L	liquid phase molar flow rate (mol/s)
n	interfacial molar flux (mol/m^{2}s)
q	heat flux (J/m^{2}s)
R	reaction rate (mol/m^{3}s)
T	temperature (K)
U	specific molar holdup (mol/m)
x	liquid phase mole fraction (mol/mol)
y	gas phase mole fraction (mol/mol)
Δz	segment height (m)
Greek letters	
δ	film thickness (m)
φ	volumetric holdup (m^3/m^3)
ξ	dimensionless film coordinate
Subscripts	
G	gas phase
L	liquid phase
i	component index
j	segment index
s	component index
t	total
Superscripts	
B	bulk
f	film
l	liquid phase
g	gas phase
I	interface
R	reaction

the reactive separation equipment is divided into several imaginary stages. These stages are linked to each other by mass and energy balances. In the case of nonequilibrium models, heat and mass is exchanged between gas and liquid phases in each stage. Mass transfer at the vapor–liquid interface is normally described using two-film model as illustrated in Fig. 1 for one stage [39–42]. In the model, it is assumed that the fluids are ideally mixed with uniform concentrations and temperatures in the bulk areas. Changes in the components molar flow in bulk region are caused either by the reactions or as a result of mass exchanges between the bulk and film sections.

Since chemical reactions take place in both phases, unsteady-state balance equations should include some reaction source terms as shown in Eqs. (1) and (2).

$$\frac{d}{dt}U_{\mathrm{L}i,j}=\frac{1}{\Delta z}\left[L_{j-1}x_{i,j-1}-L_j x_{i,j}\right]+(n^{\mathrm{B}}_{i,j}a^{\mathrm{I}}+R^{\mathrm{B}}_{\mathrm{L}i,j}\phi_{\mathrm{L}})A, \quad i=1,\ldots,n \tag{1}$$

$$U_{\mathrm{L}i,j}=x_{i,j}U_{\mathrm{L}t,j}=x_{i,j}(\phi_{\mathrm{L}}c_{\mathrm{L}t,j}A), \quad i=1,\ldots,n \tag{2}$$

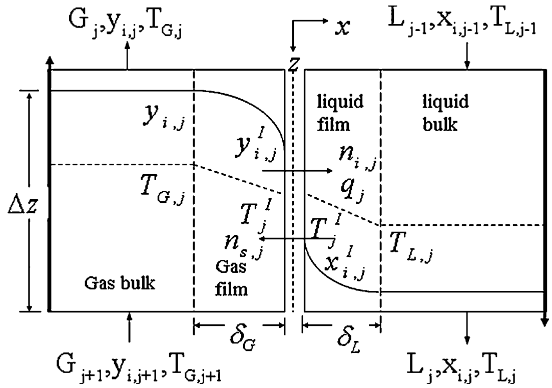

Fig. 1. Two film model in a stage of a reactive absorption packed column.

For the gas phase holdup can often be neglected due to the low gas density. Thus, the component balance for this phase is

$$0=\frac{1}{\Delta z}\left[G_{j+1}y_{i,j+1}-G_j y_{i,j}\right]-(n^{\mathrm{B}}_{i,j}a^{\mathrm{I}}-R^{\mathrm{B}}_{\mathrm{G}i,j}\phi_{\mathrm{G}})A, \quad i=1,\ldots,n \tag{3}$$

Mass balance for the components that transfer from liquid phase to gas phase is

$$0=\frac{1}{\Delta z}\left[G_{j+1}y_{s,j+1}-G_j y_{s,j}\right]+n_{s,j}a^{\mathrm{I}}A, \quad s=1,\ldots,m \tag{4}$$

To determine axial temperature profiles, energy balances are formulated including the product of the liquid molar holdup and the specific enthalpy as energy capacity. The energy balances written for continuous systems are as follows:

$$\frac{\partial E_{\mathrm{L}}}{\partial t}=-\frac{1}{\Delta z}\left[L_{j-1}h^{\mathrm{B}}_{\mathrm{L},j-1}-L_j h^{\mathrm{B}}_{\mathrm{L},j}\right]+(q^{\mathrm{B}}_{\mathrm{L}}a^{\mathrm{I}}-R^{\mathrm{B}}_{\mathrm{L}}\phi_{\mathrm{L}}\,\Delta H^{\circ}_{\mathrm{RL}})A \tag{5}$$

$$0=\frac{1}{\Delta z}\left[G_{j+1}h^{\mathrm{B}}_{\mathrm{G},j+1}-G_j h_{\mathrm{G},j}\right]-(q^{\mathrm{B}}_{\mathrm{G}}a^{\mathrm{I}}-R^{\mathrm{B}}_{\mathrm{G}}\phi_{\mathrm{G}}\,\Delta H^{\circ}_{\mathrm{RG}})A \tag{6}$$

Heat transfer rate across the vapor–liquid interface equals the sum of convective and conductive terms, the product of liquid molar holdup and the specific molar enthalpy:

$$q^{\mathrm{gf}}=-\frac{\lambda^{\mathrm{gf}}}{\delta^{\mathrm{gf}}}(T^{i}-T^{\mathrm{gb}})+\sum_{i=1}^{m}n_i^{\mathrm{gf}}h_i^{\mathrm{gf}} \tag{7}$$

$$q^{\mathrm{lf}}=-\frac{\lambda^{\mathrm{lf}}}{\delta^{\mathrm{lf}}}(T^{\mathrm{lb}}-T^{i})+\sum_{i=1}^{m}n_i^{\mathrm{lf}}h_i^{\mathrm{lf}} \tag{8}$$

The energy fluxes across the interface are linked by the continuity equation:

$$0=q^{\mathrm{gf}}-q^{\mathrm{lf}} \tag{9}$$

The summation relations connect components mole fractions in bulk liquid and gas phases:

$$\sum_{i=1}^{n}x_i^{\mathrm{B}}=1 \tag{10}$$

$$\sum_{i=1}^{n+m}y_i^{\mathrm{B}}=1 \tag{11}$$

To model unsteady-state transfer phenomena in a column segment, unsteady-state mass and heat transfer should be considered in the film and bulk regions. Unsteady-state modeling of the film leads to an initial boundary value problem as shown by Eq. (12). It has been analytically solved by Kenig et al. [42].

$$C(\xi,t)=\sum_{n=1}^{\infty}\mathrm{e}^{-[Q_n]t}\,\sin(n\pi\xi)\cdot a_n+\sum_{n=1}^{\infty}\left[\int_0^t \mathrm{e}^{-[Q_n](t-\tau)}.f_n(\tau)\,d\tau\right]\cdot\sin(\pi n\xi)+C^I(t)+\xi[C^B(t)-C^I(t)] \tag{12}$$

Diffusion coefficient has been calculated from the transformation of Maxwell–Stefan equations to the form of the generalized Fick's law. The reaction kinetic equations were linearized in the film model. In the film region, mass transfer and chemical reaction occur simultaneously. Film thickness is a parameter of the model, which needs to be estimated using empirical correlations that are available in the literature [39].

3. Determination of parameters and physical properties

The accuracy of simulation results depends on the model parameters comprising equilibrium thermodynamic, column hydrodynamics, chemical kinetics and physical properties. Phase equilibrium at the interface between phases was assumed, where interfacial compositions were calculated from the following equation:

$$y^{\mathrm{I}}_{i,j}=K_{i,j}x^{\mathrm{I}}_{i,j},\quad i=1,\ldots,n+m \tag{13}$$

where the distribution coefficient $K_{i,j}$ comprises fugacities in gas phase and activity coefficient in the liquid phase that can be determined from thermodynamic models. Reactive separation processes occur mostly in aqueous systems with electrolyte species. The well-known electrolyte models NRTL and Pitzer models are used to compute equilibrium vapor–liquid equilibrium data. In this work, to calculate equilibrium compositions at the interface a model has been used that is based on the semi-empirical Pitzer equation as reported by Krop [43]. Other parameters such as viscosities, densities and surface tension are important in calculations of mixture properties and mass transport correlations. The model parameters are presented in Table 1 as shown below. Liquid phase effective diffusion coefficients are found applying Nernst–Hartley equation, which describes transport properties in weak electrolyte systems [39]. Gas phase diffusion coefficients for low pressures are estimated by Wilke–Lee equation [47]. The influence of the process hydrodynamics are taken into the account by applying mass transfer, specific contact area, liquid holdup and pressure drop correlations [44–46].

Table 1
The list of model parameters.

Phase	Parameter	Reference
Gas	Binary diffusion coefficient	Reid et al. [47]
	Mass transfer coefficient	Onda et al. [46], Billet [45]
	Viscosity	Chapman–Enskog [47]
Liquid	Binary diffusion coefficient	Siddiqi and Lucas [55]
	Mass transfer coefficient	Onda et al. [45], Billet [44]
	Viscosity	Andrade [47]
	Surface tension	Hakim–Steniberg–Stiel [54]
	Enhancement factor	Last [52]

4. Chemical system of reactive absorption of CO_2

Reactions of carbon dioxide with amines have been extensively studied in the literature [8,11,16–18]. To model this reactive system of weak electrolytes the reactions have to be taken into the account. The reactions including CO_2 obey first and second order kinetics. Three reactions take place for CO_2; reaction between CO_2 and water, reaction between CO_2 and hydroxyl ions and reaction between CO_2 and NH_3. The first reaction to be considered is CO_2 hydration:

$$CO_2+H_2O\leftrightarrow HCO_3{}^-+H^+ \tag{14}$$

This reaction is very slow. The second reaction is bicarbonate formation:

$$CO_2+OH^-\leftrightarrow HCO_3{}^- \tag{15}$$

This reaction is fast and can enhance mass transfer even when the concentration of hydroxyl ion is low. The forward reaction can be described as below [48].

$$r_{CO_2-OH^-}=k_{OH^-}[OH^-]([CO_2]-[CO_2]_{eq}) \tag{16}$$

The primary or secondary reaction between carbon dioxide and amines leads to the formation of amine carbonate [49,50].

$$CO_2+NH_3+H_2O\leftrightarrow NH_2COO^-+H_3O^+ \tag{17}$$

The net forward rate of the reaction is

$$r_{CO_2-NH_3}=k[NH_3]([CO_2]-[CO_2]_{eq}) \tag{18}$$

where $[CO_2]_{eq}$ is CO_2 concentration in equilibrium with the local concentration of NH_3, NH_2COO^- and H_3O^+. The total rate of CO_2 reaction is

$$r_{\mathrm{overall}}=r_{CO_2-NH_3}+r_{CO_2-OH^-}+r_{CO_2-H_2O} \tag{19}$$

The rate constants that are the functions of temperature have been determined according to Danckwerts and Sharma [51].

5. Pilot plant experiments

The scheme of the absorption column pilot plant that has been used for the experimental verification of the model is shown in Fig. 2. The column is made of a 105 mm diameter glass cylinder containing four packing sections. A tray is mounted between these sections to redistribute the liquid flow. On each tray, two temperature sensors and two valves were installed to measure gas and liquid temperatures as well as taking liquid and gas samples, respectively. The height of each packing section was 650 mm. The packing beads were ceramic Rashing rings with diameter of 0.5 in. Gas and liquid samples were taken at five points of the column as shown in Fig. 2. Temperatures were measured at five positions along the column to give temperature profiles for gas and liquid phases.

6. Numerical solution

The process model was a set of partial and ordinary differential equations. The equations were discretized in axial direction (column height) using the method of lines resulting in a system of coupled ODEs and algebraic equations. The column was divided to 100 stages. The algorithm of model equations solution is shown in Fig. 3. The film model was solved using analytical method that is much faster than numerical solution.

7. Experimental and analytical methods

The experimental data were obtained in steady-state conditions. At the beginning of each experiment, only nitrogen gas was fed to

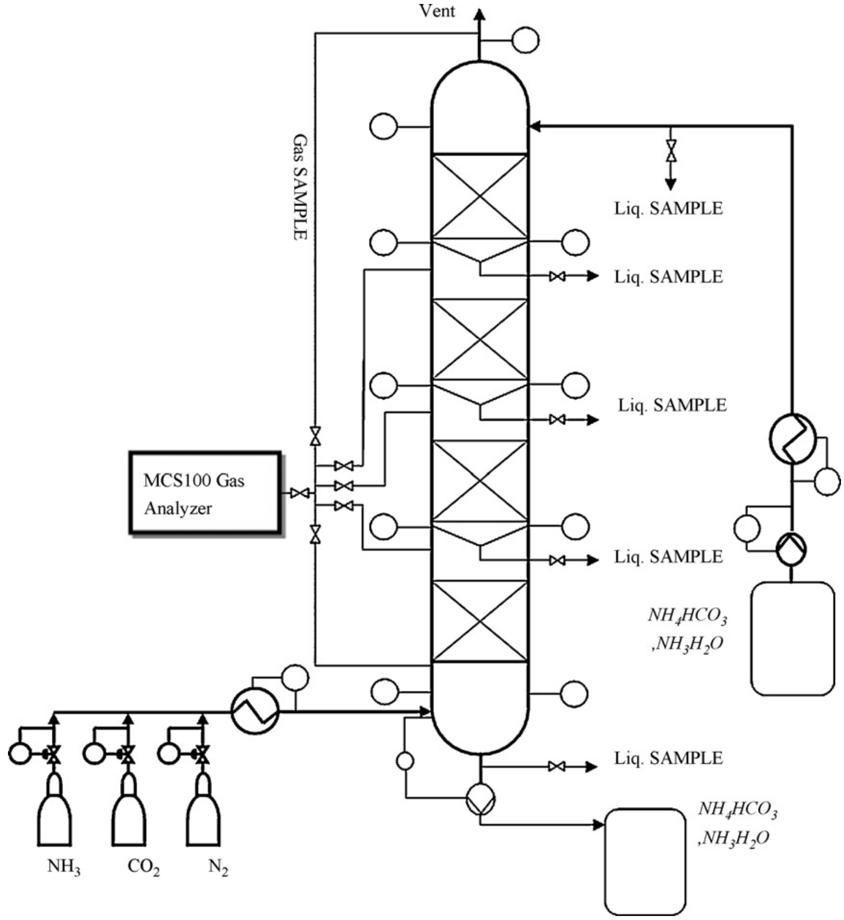

Fig. 2. Scheme of the absorption pilot plant.

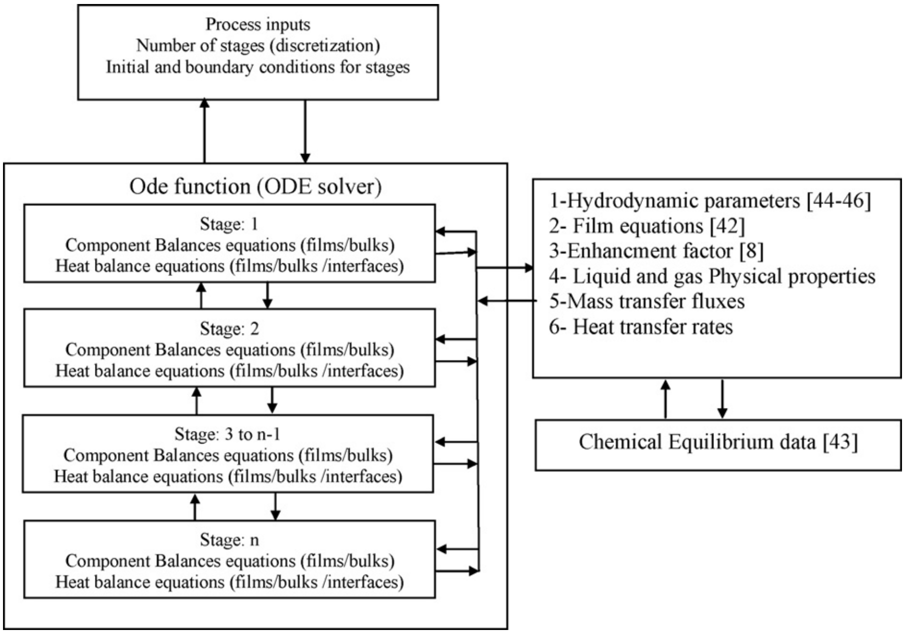

Fig. 3. The algorithm of model equations solution using the method of lines.

Table 2
Operating conditions of absorption column.

Process variables	Feed	Outlet
Gas		
Temperature [°C]	25.2	31.9
NH_3 [mol/h]	0	2.21
CO_2 [mol/h]	41.94	27.0
N_2 [mol/h]	195.7	195.7
H_2O [mol/h]	0	14.3
Liquid		
Temperature [°C]	31.1	32.3
NH_3 [mol/m^3]	1036.9	1020.5
CO_2 [mol/m^3]	380.7	505.2

the column then liquid and other gas feed flow rates and temperatures were adjusted to the desired values. Gas and liquid samples were taken after reaching steady-state conditions, which was indicated by a steady-state temperature profile and fixed concentration of the analyzer. Duplicate liquid and gas samples were taken with a time interval of about 10 min.

The liquid samples were analyzed offline, using an ion chromatography (IC-762 type from Metrohm company) based on conductivity detection method. The gas samples were analyzed by an online gas analyzer, MCS100 (from SICKMAIHAK Company), which is an extremely compact multi-component infrared photometer for extractive continuous monitoring of flue gases. In this process H_2O, NH_3 and CO_2 concentrations were measured in five different positions of the column as illustrated in Fig. 2. The time response of MCS100 is less than 2 s. The temperature sensors precision is about 0.1 K. Pilot plant experiments have been carried out with different liquid phase concentrations and at the same liquid phase flow rate of 120 l/h. Inlet and outlet experimental conditions of the absorption column are shown in Table 2. The absorption column is operated in atmospheric pressure.

8. Results and discussion

CO_2 absorption by partially carbonated ammonia solution has been carried out in the pilot plant. The film model equations could be solved both analytically and numerically. Fig. 4 shows the results of numerical and analytical solutions of film equations for different times of the experiment from 0.0001 to 0.1 s. This figure indicates that CO_2 concentration changes with time, which justifies the use of a dynamic model for the film region.

Fig. 5 shows the variation of CO_2 flux against film coordinate. At the interface of the film, CO_2 absorption rate has also been calculated using enhancement factor. These results indicate using enhancement factor leads to absolute relative error of 6.7 present for calculation of CO_2 absorption rate compared to the value obtained from analytical solution. The figure displays a good agreement between numerical and analytical solutions using film model.

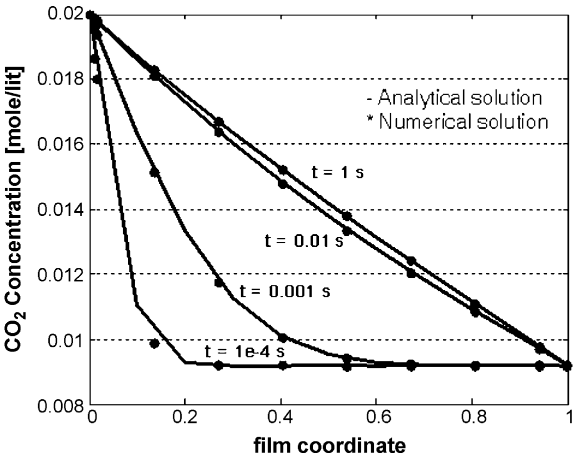

Fig. 4. CO_2 concentration gradients in film coordinate at different time.

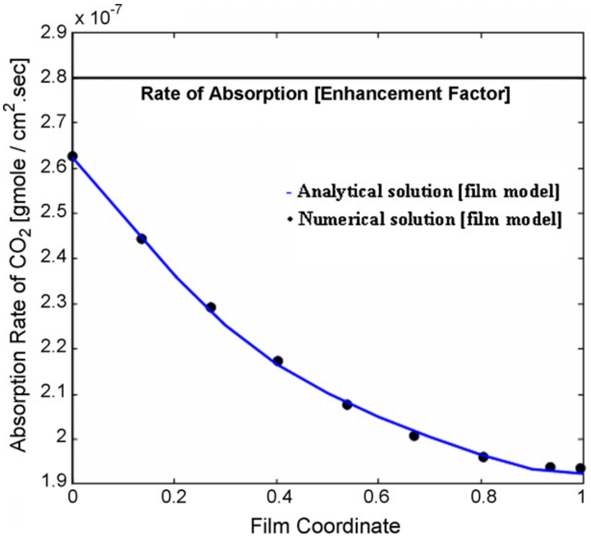

Fig. 5. CO_2 absorption rate against film coordinate using either dynamic film model or enhancement factor in an arbitrary section of the column.

Table 3 shows temperatures and components concentrations along the column in steady-state condition. The results of this table indicate that there is no H_2O and NH_3 in the gas feed although when the gas phase enters the column its H_2O and NH_3 content starts to rise due to the mass transfer from liquid phase to gas phase.

In Fig. 6, gas phase components gradient has been presented. Only molecular components (NH_3, H_2O, CO_2 and N_2) exist in the gas phase whereas the liquid phase contains nine ion and molecular components. Fig. 6 indicates that CO_2 mole fraction decreases along the column height due to its absorption, whereas NH_3 and H_2O concentrations increase as a result of mass transfer from liquid phase to the gas. Since the sum of all mole fractions equals 1, N_2 concentration curve is descending at the bottom section of the column and ascending at other sections as a result of the variations in the concentrations of other components in the gas phase.

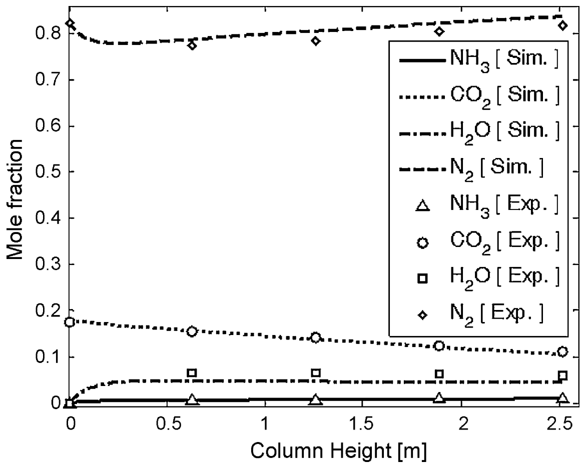

Fig. 6. Gas phase mole fractions of components over the column height.

Table 3
Pilot plant experimental data of concentrations and temperatures in steady-state condition.

Section height	Gases mole fractions [pressure/total pressure]				Temperature [K]		Liquid concentration [mole/m^3]	
Z [m]	N_2	CO_2	NH_3	H_2O	T_G	T_L	NH_3	CO_2
2.60	0.818	0.113	0.0092	0.060	31.9	31.1	1038.9	380.7
1.95	0.804	0.125	0.0089	0.062	32.3	31.5	1036.7	409.5
1.30	0.785	0.143	0.008	0.065	32.9	32.0	1032.8	451.9
0.65	0.773	0.154	0.0066	0.066	33.2	32.6	1030.9	480.9
0	0.824	0.177	0	0	25.2	32.3	1020.5	505.2

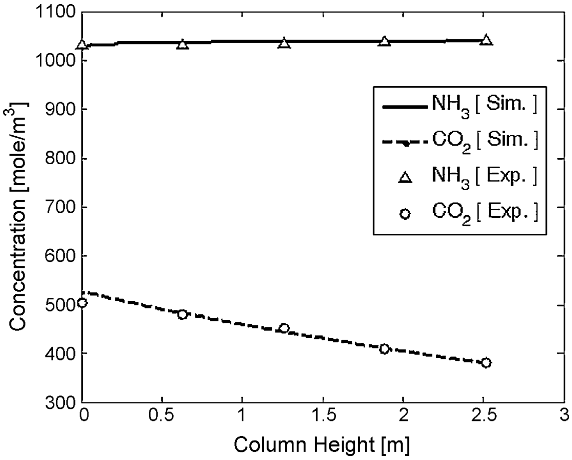

Fig. 7. Concentration profiles of electrolyte components in the liquid phase along the column height.

In the liquid phase, concentrations of electrolytes (NH_3, CO_2) were determined by these equations:

$$NH_3 = [NH_3] + [NH_2COO^-] + [NH_4^+] \tag{20}$$

$$CO_2 = [CO_2] + [NH_2COO^-] + [HCO_3^-] + [CO_3^{2-}] \tag{21}$$

Fig. 7 shows that along the column height total CO_2 concentration increases due to its absorption in the solution whereas mass transfer of NH_3 from liquid phase to gas phase causes total NH_3 concentration to decrease slightly.

Since CO_2 absorption is an exothermic process, solution temperature increases along the column. Fig. 8 shows temperature gradients in both phases. In the lower section of the column the heat transfers from liquid to the gas phase, whereas in other sections it is vice versa.

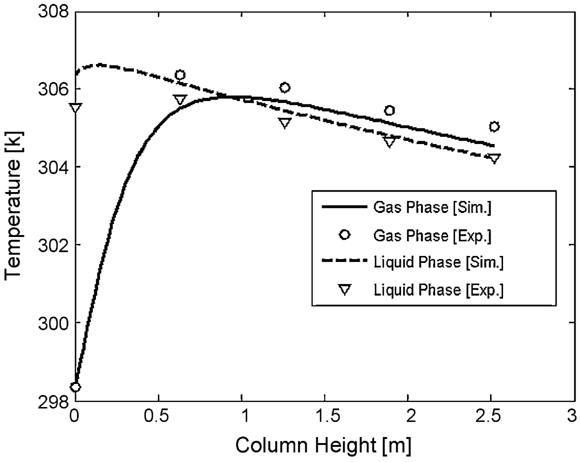

Fig. 8. Temperature gradients in liquid and gas phases along the column height.

Simulation results of this model have been compared with those of enhancement factor model (a model using enhancement factor). Several researches have been conducted on enhancement factor for reactive absorption of CO_2 by solutions [8,4,51,52]. In this research, both methods of film model and enhancement factor approach are applied for unsteady-state mass transfer conditions. Unsteady-state diffusion results in initial boundary value problem (IBVP). "When using the film model, IBVP problem has been solved analytically by Kenig et al. with real initial and boundary conditions whereas when using enhancement factor approach the IBVP problem has been solved with simplified conditions (the concentration at initial condition and in liquid bulk are considered to be zero). Therefore, unreal conditions of enhancement factor approach result in more absorption rate than real absorption rate. The factor used in this research, has been presented by Last [52] as follows:

$$E = \sqrt{1 + Ha^2}$$

where Ha is Hatta number as follow:

$$Ha = \frac{\sqrt{k_2 D_{CO_2}[NH_3]}}{k_L}$$

Absorption rate of CO_2 in partially carbonated ammonia based on both methods have been shown in Fig. 5 for an arbitrary section. The comparison of both methods shows that film models are more rigorous than enhancement factor approach.

In this work relative deviation (RD) has been used as a criterion to compare the models. RD has been calculated using Eq. (22).

$$RD\% = \frac{\left|X_{Exp.} - X_{Cal}\right|}{X_{Exp.}} \times 100 \tag{22}$$

where X_{Exp} is experimental and X_{Pre} is a predicted value by one of the models.

Comparing RDs of the models given in Table 4 revealed that film models resulted in higher accuracy than enhancement factor models.

Since the process model is dynamic, it can produce unsteady simulation results such as dynamic variations of total CO_2 concentration and liquid temperature. Fig. 9 shows CO_2 concentration

Table 4
Simulation results and experimental data of temperatures and concentrations.

Process variables	Exp. data	Model based on film model		Enhancement factor model	
		Simulation	RD%	Simulation	RD%
Outlet liquid					
T_L	305.45	306.37	0.3	307.723	0.74
NH_3	1020.5	1024.85	0.40	1027.7	0.7
CO_2	505.2	523.4	3.60	594.9	17.76
Outlet gas					
T_G	305.05	304.543	0.17	304.741	0.1
NH_3	0.0092	0.0108	17.4	0.0107	16.3
CO_2	0.113	0.1072	5.13	0.0691	38.8
H_2O	0.06	0.0445	25	0.0446	25.7
N_2	0.818	0.8375	2.38	0.8756	7.0

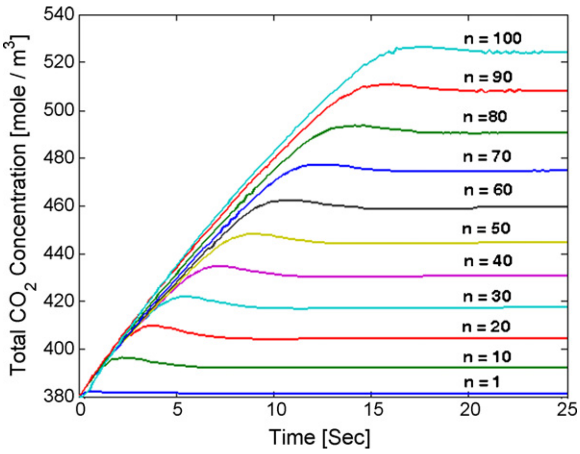

Fig. 9. Dynamic variation of liquid total CO_2 concentration in different column stages.

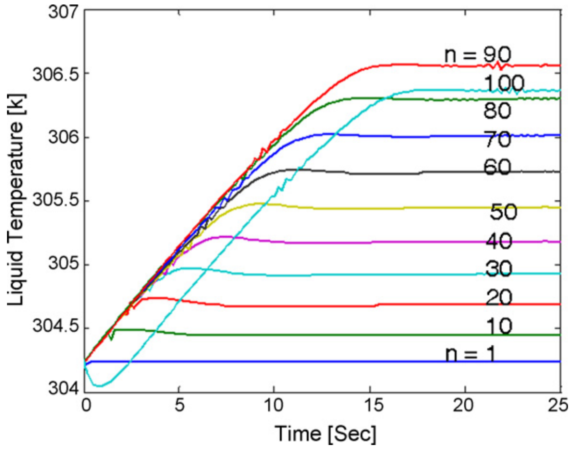

Fig. 10. Dynamic variation of solution temperature in stages along the column.

in different numerical stages. It also displays that CO_2 has been absorbed in liquid phase gradually throughout the column. In this figure, *n* is stage number, where stage 1 is at the top of the column and stage 100 is at the bottom.

Fig. 10 shows dynamic variation of liquid temperature along the column. It indicates that at the bottom of the column due to heat transfer from liquid phase to gas phase the liquid temperature is descending. Therefore, steady-state temperature at the 100th stage is lower than that of 90th stage.

9. Conclusions

In this work, a nonequilibrium model that takes heat and mass transfer into the account in both phases has been introduced to describe reactive separation processes especially reactive absorption of CO_2 into aqueous carbonated ammonia solution. The model has been validated against experimental data that have been obtained employing a pilot plant. A comparison between experimental and simulation results showed that the agreement of simulation predictions and experiments data of temperature and concentration follow the same trends. The model developed in this study can predict mole fraction and concentration of all components that exist in liquid and gas phases along the column in both steady-state and dynamic conditions. A comparison between simulation results, obtained using enhancement factor and film model, with experimental data revealed that the model predicts the process with less error when film model has been used.

References

[1] A.L. Kohl, F.C. Riesenfeld, Gas Purification, Gulf Publication Co., Houston, Texas, 1985.
[2] G. Sartori, D.W. Savage, Satirically hindered amines for CO_2 removal from gases, Ind. Eng. Chem. Fundam. 22 (1983) 239–249.
[3] A.M. Worlesky, E.J. Daniels, B.J. Jody, CO_2 capture from the flue gas of conventional fossil-fuel fired power plants, Environ. Prog. 13 (1994) 214–219.
[4] S. Masuda, Chemical CO_2 fixation technology—RITE projects, Energy Conserv. Manage. 36 (1995) 567–572.
[5] H. Michiki, Biological CO_2 fixation and utilization project, Energy Conserv. Manage. 36 (1995) 701–706.
[6] N. Kimura, K. Omata, T. Kiga, S. Takano, S. Shikisima, The characteristics of pulverized coal combustion in O_2/CO_2 mixture for recovery, Energy Conserv. Manage. 36 (1995) 805–808.
[7] H.B. Al-Saffar, J.S. Oklany, K. Ozturk, R. Hughes, Removal of carbon dioxide from gas streams using a gas/liquid hollow fiber module, Trans. Inst. Chem. Eng. 73 (1995) 144–150.
[8] P.V. Danckwerts, Gas/Liquid Reactions, McGraw-Hill, New York, 1970.
[9] R. Maceiras, E. Alvarez, M. Angeles, Effect of temperature on carbon dioxide absorption in monoethanolamine solutions, Chem. Eng. J. 138 (2008) 295–300.
[10] L. Jiun-Jie, K. Meng-Hui, Kinetics of absorption of carbon dioxide into solutions of *N*-methyldiethanolamine+water, Chem. Eng. Sci. 55 (2000) 4139–4147.
[11] S. Wei-Chen, Y. Chia-Bao, L. Meng-Hui, Kinetics of the absorption of carbon dioxide into mixed aqueous solutions of 2-amino-2-methyl-l-propanol and piperazine, Chem. Eng. Sci. 60 (2005) 503–516.
[12] B.P. Mandal, M. Guha, A.K. Biswas, S.S. Bandyopadhyay, Removal of carbon dioxide by absorption in mixed amines: modeling of absorption in aqueous MDEA/MEA and AMP/MEA solutions, Chem. Eng. Sci. 56 (2001) 6217–6224.
[13] M.K. Aroua, M.Z. Haji-Sulaiman, K. Ramasamy, modeling of carbon dioxide absorption in aqueous solutions of AMP and MDEA and their blends using Aspen plus, Sep. Purif. Technol. 29 (2002) 153–162.
[14] H.L. Sheng, T.S. Ching, Performance characteristics and modeling of carbon dioxide absorption by amines in a packed column, Waste Manage. 19 (1999) 255–262.
[15] S. Schubert, M. Grünewald, D.W. Agar, Enhancement of carbon dioxide absorption into aqueous methyldiethanolamine using immobilised activators, Chem. Eng. Sci. 56 (2001) 6211–6216.
[16] X. Zhang, S. Schubert, M. Gruenewald, D.W. Agar, Studies on the kinetics of carbon dioxide absorption with immobilised amines (IA), Chem. Eng. J. 107 (2005) 97–102.
[17] L. Chen-Hung, L. Meng-Hui, Kinetics of absorption of carbon dioxide into aqueous solutions of monoethanolamine + *N*-methyldiethanolamine, Chem. Eng. Sci. 57 (2002) 4569–4582.
[18] J. Yoon, J. Baek, Y. Yamamoto, T. Komai, T. Kawamura, Kinetics of removal of carbon dioxide by aqueous 2-amino-2-methyl-1,3-propanediol, Chem. Eng. Sci. 58 (2003) 5229–5237.
[19] S. Van Loo, E.P. van Elk, G.F. Versteeg, The removal of carbon dioxide with activated solutions of methyl-diethanol-amine, J. Petrol Sci. Eng. 55 (2007) 135–145.
[20] M.S. Sivasubramanian, R. Taylor, R. Krishnamurthy, A nonequilibrium stage model of multicomponent separation processes. Part IV. A novel approach to packed column design, AIChE J. 33 (1987) 325–327.
[21] E.J. Henley, J.D. Seader, Equilibrium Stage Separation Operations in Chemical Engineering, Wiley, New York, 1981.
[22] J.D. Seader, The rate-based approach for modeling staged separations, Chem. Eng. Progr. 85 (1989) 41–49.
[23] R. Taylor, H.A. Kooijman, M.R. Woodman, Industrial applications of a nonequilibrium model of distillation and absorption operations, Inst. Chem. Eng. Symp. Ser. 128 (1992) A415–A427.
[24] R. Taylor, H.A. Kooijman, J.S. Hung, A 2nd generation nonequilibrium model for computer-simulation of multicomponent separation processes, Comput. Chem. Eng. 18 (1994) 205–217.
[25] E.Y. Kenig, A. Gorak, A film model based approach for simulation of multicomponent reactive separation, Chem. Eng. Process. 34 (1995) 97–103.
[26] E.Y. Kenig, L. Kucka, A. Gorak, Rigorous modeling of reactive absorption processes, Chem. Eng. Technol. 26 (2003) 631–646.
[27] M. Kloeker, E.Y. Kenig, A. Hoffmann, P. Kreis, A. Gorak, Rate-based modelling and simulation of reactive separations in gas/vapour–liquid systems, Chem. Eng. Process. 44 (2005) 617–629.
[28] S. Pelkonen, A. Gorak, H.A. Kooijman, R. Taylor, Operation of a packed distillation column: modelling and experiments, I. Chem. E. Symp. Ser., Maastricht, NL (1997).
[29] N. Asprion, Nonequilibrium rate-based simulation of reactive systems: simulation model. Heat transfer, and influence of film discretization, Ind. Eng. Chem. Res. 45 (2006) 2054–2069.
[30] R. Schneider, F. Sander, A. Gorak, Dynamic simulation of industrial reactive absorption processes, Chem. Eng. Process. 42 (2003) 955–964.

[31] O. Brettschneider, R. Thiele, R. Faber, H. Thielert, G. Wozny, Experimental investigation and simulation of the chemical absorption in a packed column for the system NH3–CO_2–H_2S–NaOH–H_2O, Sep. Purif. Technol. 39 (2004) 139–159.

[32] L. Kucka, I. Muller, E.Y. Kenig, A. Groak, On the modeling and simulation of sure gas absorption by aqueous amine solutions, Chem. Eng. Sci. 58 (2003) 2571–3578.

[33] A. Higler, R. Taylor, R. Krishna, Modeling of a reactive separation process using a nonequilibrium stage model, Comput. Chem. Eng. 22 (1998) S111–S118.

[34] R. Krishnamurthy, R. Taylor, A nonequilibrium stage model of multicomponent separation processes. Part I. Model description and method of solution, AIChE J. 31 (1985) 449–456.

[35] R. Krishnamurthy, R. Taylor, A nonequilibrium stage model of multicomponent separation processes. Part II: comparison with experiment, AIChE J. 31 (1985) 456–465.

[36] R. Krishnamurthy, R. Taylor, A nonequilibrium stage model of multicomponent separation processes. Part III: the influence of unequal component efficiencies in process design problems, AIChE J. 31 (1985) 1973–1985.

[37] R. Krishnamurthy, R. Taylor, Simulation of packed distillation and absorption columns, Ind. Eng. Chem. Proc. Des. Dev. 24 (1985) 513–524.

[38] R. Krishnamurthy, R. Taylor, Absorber simulation and design using a nonequilibrium stage model, Can. J. Chem. Eng. 64 (1986) 96–105.

[39] R. Taylor, R. Krishna, Multicomponent Mass Transfer, Wiley, New York, 1993.

[40] E.Y. Kenig, F. Butzmann, L. Kucka, A. Gorak, Comparison of numerical and analytical solutions of a multicomponent reaction-mass-transfer problem in terms, Chem. Eng. Sci. 55 (2000) 1483–1496.

[41] C. Noeres, E.Y. Kenig, A. Gorak, Modeling of reactive separation processes: reactive absorption and reactive distillation, Chem. Eng. Process. 42 (2003) 157–178.

[42] E.Y. Kenig, R. Schneider, A. Gorak, Multicomponent unsteady-state film model: a general analytical solution to the linearized diffusion–reaction problem, Chem. Eng. J. 83 (2001) 85–94.

[43] J. Krop, New approach to simplify the equation for the excess Gibbs free energy of aqueous solution of electrolytes applied to the modeling of the NH_3–CO_2–H_2O vapor–liquid equilibria, Fluid Phase Equilib. 163 (1999) 209–229.

[44] R. Billet, M. Schultes, Mass Transfer in Gas/Liquid Systems, in: Presented at AIChE Annual Meeting, Washington DC, USA, 1988.

[45] R. Billet, Packed Towers in Processing and Environmental Technology, VCH, Weinheim, 1995.

[46] K. Onda, H. Takeuch, Y. Okumoto, Transfer coefficient between gas and liquid phase in packed columns, J. Eng. Jpn. 1 (1968) 56–61.

[47] R.C. Reid, J.M. Prausnitz, B.E. Poling, The Properties of Gases and Liquids, McGraw-Hill, New York, 1987.

[48] B.R.W. Pinsent, L. Pearson, F.W.J. Roughton, The kinetics of combination of carbon dioxide with hydroxide ions, Trans. Farad. Soc. 52 (1956) 1512–1520.

[49] D.M. Clark, Rafal, N.C. Scrivner, Handbook of Aqueous Electrolyte Thermodynamics, AIChE, New York, USA, 1986, pp. 606–608.

[50] J. Shen, Y. Yang, J. Maa, Promotion mechanism for CO_2 absorption into partially carbonated ammonia solutions, J. Chem. Eng. Jpn. 32 (1999) 378–381.

[51] P.V. Danckwerts, M.M. Sharma, The absorption of carbon dioxide into solutions of alkalis and amines, Chem. Eng. (1966) CE244–CE280.

[52] W. Last, J. Stichlmair, Determination of mass transfer parameters by means of chemical absorption, Chem. Eng. Technol. 25 (2002) 385–391.

[54] Aspen, Aspen Properties. Physical property methods and models, version 10.2, Aspen Technology, Inc., Cambridge, MA, USA, 2000.

[55] M.A. Siddiqi, K. Lucas, Correlations for prediction of diffusion in liquids, Can. J. Chem. Eng. 64 (1986) 839–843.